Control and removal of modulational instabilities in low-dispersion photonic crystal fiber cavities

M. Tlidi

Optique Nonlineaire Theorique Université Libre de Bruxelles, C.P. 231, Campus Plaine, B-1050 Bruxelles, Belgium

A. Mussot and E. Louvergneaux

Laboratoire de Physique des Lasers, Atomes et Molecules, UMR-CNRS 8523 IRCICA, Université des Sciences et Technologies de Lille, 59655 Villenueve d'Ascq Cedex, France

G. Kozyreff

Optique Nonlineaire Theorique Université Libre de Bruxelles, C.P. 231, Campus Plaine, B-1050 Bruxelles, Belgium

A. G. Vladimirov

Weierstrass Institute for Applied Analysis and Stochastics, Mohrenstrasse 39, D-101178 Berlin, Germany

M. Taki

Laboratoire de Physique des Lasers, Atomes et Molecules, UMR-CNRS 8523 IRCICA, Université des Sciences et Technologies de Lille, 59655 Villenueve d'Ascq Cedex, France

Received October 11, 2006; accepted November 29, 2006;
posted December 20, 2006 (Doc. ID 75864); published February 15, 2007

Taking up to fourth-order dispersion effects into account, we show that fiber resonators become stable for a large intensity regime. The range of pump intensities leading to modulational instability becomes finite and controllable. Moreover, by computing analytically the thresholds and frequencies of these instabilities, we demonstrate the existence of a new unstable frequency at the primary threshold. This frequency exists for an arbitrary small but nonzero fourth-order dispersion coefficient. Numerical simulations for a low and flattened dispersion photonic crystal fiber resonator confirm analytical predictions and open the way to experimental implementation. © 2007 Optical Society of America

OCIS codes: 190.0190, 190.3100, 190.4360, 190.4370, 230.4320.

Instabilities in nonequilibrium systems are drawing considerable attention both from fundamental as well as applied point of views.[1,2] One such instability gives rise to periodic self-modulations and is referred to as modulational instability (MI) in temporally dispersive media[3] and Turing instability[4] in spatially extended systems. In optical fibers, MI results from the interplay between chromatic dispersion and the intensity-dependent refractive index. In the usual scalar-free propagation, the phase matching of the underlying four-wave mixing process requires anomalous dispersion.[3] However, phase matching can also be achieved in normal dispersion region by considering extra degrees of freedom such as polarization in birefringent[5] and isotropic[6] fibers, bimodal fibers,[7] working around the zero-dispersion wavelength (ZDW),[8–10] or inserting the fiber within a cavity.[11] Scalar MI in free propagation through a single-mode optical fiber is usually described by the nonlinear Schrödinger equation (NLSE), in which the propagation constant is expanded in a Taylor series in the frequency domain. It has been shown that only even-order terms contribute to the MI gain and that development up to the fourth order must be considered when the pump wavelength is close to the ZDW. In this case, scalar MI is possible in the normal dispersion region if the fourth-order dispersion term is negative, and a second frequency of instability can be generated if the fourth-order dispersion term is positive.[8–10] To our knowledge, intracavity MI leading to a single frequency has been studied only in relatively strong dispersion regions where models including up to the second-order dispersion term are relevant to describe its dynamics.

In this Letter, we show that it is necessary to take into account up to the fourth-order dispersion term to capture the full MI dynamics of a passive fiber resonator, especially when proceeding close to the ZDW. To this end, we extend the model developed by Lugiato–Lefever[12] (LL model) up to the fourth-order dispersion term. We then demonstrate that, however small the fourth-order dispersion coefficient is, a second frequency of instability can be observed at the primary threshold of stationary state destabilization, which adds to the single frequency predicted and observed up to now.[11] Moreover, we demonstrate that the MI process has a finite domain of existence delimited by two pump power values, allowing for the stationary state to restabilize at large powers. We investigate the evolution of the MI frequencies within the

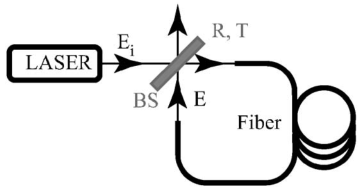

Fig. 1. Experimental setup. BS, beam splitter.

existence domain from their rise up to their disappearance. Finally, in view of an experimental implementation, we perform numerical simulations for a realistic experimental configuration with a flattened dispersion photonic crystal fiber and find excellent agreement with the analytical predictions.

The fiber resonator is schematically depicted in Fig. 1. A continuous wave of power E_i^2 is launched into the cavity by means of a beam splitter, propagates inside the fiber, and experiences dispersion and the Kerr effect. At each round trip the light inside the fiber is coherently superimposed with the input beam. This can be described by the boundary conditions $E(z=0,\tau+t_R)=T\times E_{in}(\tau)+R\times E(L,\tau)\exp(-i\Phi_0)$ and by the extended NLSE $\partial_z E(z,\tau)=(-i\beta_2/2\partial_{\tau^2}+\beta_3/6\partial_{\tau^3}+i\beta_4/24\partial_{\tau^4}+i\gamma|E|^2)E$, with round-trip time t_R, linear phase shift Φ_0, intensity mirror transmissivity (reflectivity) T^2 (R^2), and cavity length L. The electric field inside the cavity is denoted E. $\beta_{2,3,4}$ are the second-, third-, and fourth-order dispersion terms, respectively. γ is the nonlinear coefficient, z is the longitudinal coordinate, and τ is the time in a reference frame moving at the group velocity of the light. This infinite-dimensional map can be simplified to the following single normalized equation by applying the mean field approximation:

$$\frac{\partial\psi}{\partial t'}=S-(1+i\Delta)\psi+i|\psi|^2\psi-i\beta_2\frac{\partial^2\psi}{\partial\tau'^2}+B_3\frac{\partial^3\psi}{\partial\tau'^3}+iB_4\frac{\partial^4\psi}{\partial\tau'^4}, \quad (1)$$

where $t'=tT^2/2t_R$, $\tau'=\tau(T^2/L)^{1/2}$, $\psi=E\sqrt{2\gamma L/T^2}$, $S=2/T(2\gamma L/T^2)^{1/2}E_i$ is the normalized input field, $B_3=\beta_3 T/\sqrt{9L}$, $B_4=\beta_4 T^2/12L$, and $\Delta=2\Phi_0/T^2$ is the cavity detuning. We carry out the analytical study in a low-dispersion fiber with a small dispersion slope. Thus, B_3 can be neglected. The steady state (SS) response ψ_S of Eq. (1) satisfies $S_S=[1+i(\Delta-|\psi_S|^2)]\psi_S$. This solution is identical to that of the LL model leading to a monostable (bistable) regime for $\Delta<\sqrt{3}$ ($>\sqrt{3}$). Its stability with respect to finite frequency perturbations, i.e., of the form $\exp(i\Omega\tau'+\lambda t')$, shows that the MI frequencies that can be destabilized at the primary threshold $I_{1m}=|\psi_{1m}|^2=1$ are

$$\Omega_{L,U}^2=\frac{-\beta_2\pm\sqrt{\beta_2^2+4(\Delta-2)B_4}}{2B_4}, \quad (2)$$

and one can see immediately that two frequencies can be destabilized at the primary threshold for a suitable choice of β_2 and Δ. Thus, taking into account β expansion up to the fourth order in Eq. (1) evidences the existence of a second frequency of instability that has not yet been reported experimentally or theoretically when working in quite strong dispersion regions.[11]

This result is illustrated by the closed marginal stability curve in Fig. 2(a), where two destabilization frequencies (Ω_L and Ω_U) exist at the primary threshold I_{1m} in the monostable regime [Fig. 2(b)]. The finite extent of the MI domain is also evidenced by the lower and upper values of cavity power, $|\psi_{1m}|^2=I_{1m}=1$ and $|\psi_{2m}|^2=I_{2m}=(2\Delta_{eff}+\sqrt{\Delta_{eff}^2-3})/3$. The lower value fixes the minimum input power required for the MI process to occur, while the upper one can be tuned as a function of the physical parameter $\Delta_{eff}=\beta_2^2/(4B_4)+\Delta$. The critical value of the frequency at the upper bifurcation point I_{2m} is given by $\Omega_c^2=-\beta_2/2B_4$, and we note that it satisfies the averaging relation $\Omega_c^2=\Omega_L^2+\Omega_U^2$. This result strongly contrasts with the usual cavity MI where the instability domain is not bounded as shown in Fig. 2(a) by the gray curves. So the two main results of this stability analysis are that (i) two instabilities at frequencies Ω_U and Ω_L occur simultaneously at the primary threshold (I_{1m}) and (ii) it is possible to restabilize or recover the stationary state by driving the system to the large intensity regime ($I>I_{2m}$).

In view of the above analysis, an important question arises: how do the first two frequencies Ω_L and Ω_U evolve and connect to Ω_c upon increasing the input intensity $P=|S|^2$? The linear stability analysis can give us some insight on this point through the evolution of the most unstable frequencies of the SS,

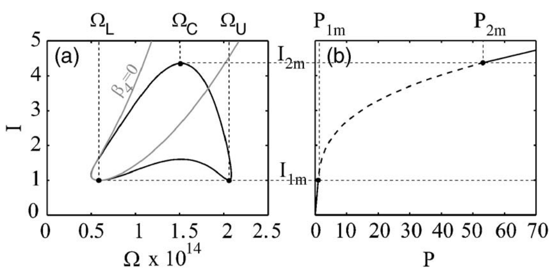

Fig. 2. (a) Marginal stability curve for the steady state solution versus MI. Black curve, $\beta_4\neq 0$; gray curve, $\beta_4=0$. (b) Evolution of the cavity intensity stationary state $I=|\psi_S|^2$ versus the input intensity $P=|S|^2$ (the dashed curve corresponds to the unstable case). $\gamma=10\ \mathrm{W^{-1}\,km^{-1}}$, $\Phi_0=1.98\pi$, $T=0.35$, $L=10$ m, $\beta_2=-3\times10^{-28}\ \mathrm{s^2/m}$, $\beta_3=0$, $\beta_4=6.4\times10^{-54}\ \mathrm{s^4/m}$.

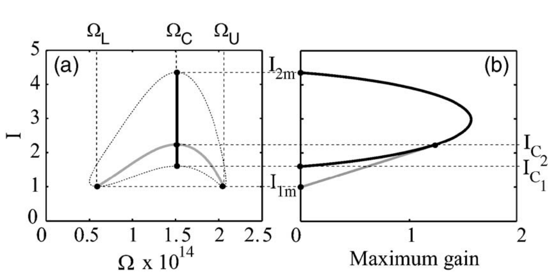

Fig. 3. Evolution of the maximum temporal gains (solid black and gray lines) versus (a) the frequency Ω and (b) the output intensity I.

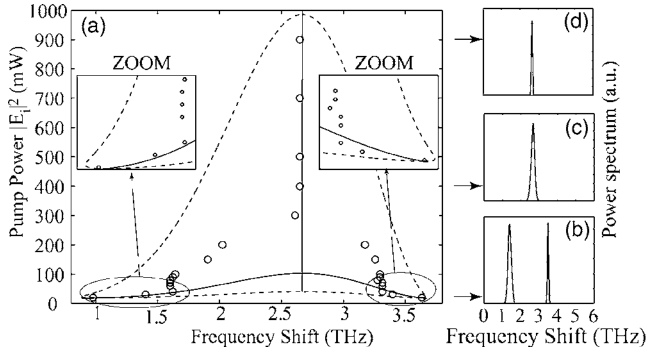

Fig. 4. (a) Evolution of the frequency of instability versus the pump power with the same parameters as in Fig. 2, except for $\beta_3 = 2\times10^{-42}$ s^3/m. Circles, numerical simulations; solid curves, analytical results. (b), (c), and (d) power spectra for 30, 400, and 900 mW of pump power, respectively.

as shown in Fig. 3. At $I \geqslant 1$ the SS undergoes a bifurcation leading to small-amplitude modulations at frequencies Ω_L and Ω_U. The two corresponding bands of unstable frequencies widen with growing I until it reaches the value I_{c1} at $\Omega = \Omega_c$ [Fig. 3(a)]. This signals the merging of the two bands into a single larger one. This new band of unstable frequencies is now characterized by the existence of three frequencies with positive gain, as can be seen from Fig. 4(b). When we further increase I, the two most unstable lateral frequencies merge into the critical one Ω_c at $I = I_{c2}$. This point indicates an outstanding feature leading to an exchange of the maximum gain between Ω_L (Ω_U) and Ω_c [Fig. 3(b)]. Finally, one then can expect from Fig. 3 that above this power value ($I > I_{c2}$) the dynamics is dominated by the frequency Ω_c until the upper limit of the instability domain is reached ($I = I_{2m}$).

These results should be experimentally observable using a fiber whose dispersion curve is low and as flat as possible at the working wavelength ($\beta_3 \approx 0$). We numerically checked our predictions by integrating the extended NLSE with bounded conditions by using the split-step Fourier method with an input continuous wave. We included realistic third- and fourth-order dispersion term values in our simulations (see the caption of Fig. 2). Indeed, we did not take exactly $\beta_3 = 0$ but a very low value [$D_S = 0.001$ ps/nm^2/km, i.e., $\beta_3 = 2\times10^{-42}$ s^3/m (Ref. 13)] to match with a realistic configuration. We have checked in all our simulations that the final state was reached ($\simeq 400$ round trips). We show in Fig. 4(a) that two frequencies (0.98 and 3.63 THz) are destabilized (circles) just above the first pump threshold (20 mW) [Fig. 4(b)], in excellent agreement with the analytical results (1.1 and 3.6 THz). Upon increasing the pump power, the frequencies merge, leading to a single frequency of instability around 300 mW [Fig. 4(c)]. This unique frequency then disappears just above the second pump threshold, corresponding to a recovery of the stationary state of the cavity. Thus, the two main predictions of our analytical study are numerically verified. This linear stability analysis provides an excellent insight into the frequency evolution scenario within the instability domain, except for 50 mW $< I <$ 300 mW [Fig. 4(a)]. In this last region only a nonlinear analysis as in Refs. 14 and 15 will figure out the dynamic evolution of the system. This work is in progress.

To summarize, we presented an analytical and numerical study of a coherently driven photonic crystal fiber resonator. We showed that it is necessary to take into account dispersion up to the fourth order to capture the full temporal dynamics of the system. Namely, there exist two frequencies at the primary MI threshold, and their domain of existence is finite or bounded such that the stationary state is recovered for pumping of high enough intensity. In addition, numerical simulations carried out for realistic experimental parameters provide the evolution of these instabilities with the input field. They confirm our analytical results and constitute a step towards a future experimental demonstration.

M. Tlidi (mtlidi@ulb.ac.be) and G. Kozyreff received support from the Fonds National de la Recherche Scientifique (Belgium). This work was also partially supported by the Interuniversity Attraction Pole program of the Belgian government. The IRCICA and CERLA are supported in part by the "Conseil Régional Nord Pas de Calais" and the "Fonds Européen de Développement Economique des Régions."

References

1. M. C. Cross and P. C. Hohenberg, Rev. Mod. Phys. **65**, 851 (1993).
2. G. P. Agrawal, *Nonlinear Fiber Optics* (Academic, 1995).
3. K. Taï, A. Hasegawa, and A. Tomita, Phys. Rev. Lett. **56**, 135 (1986).
4. A. M. Turing, Philos. Trans. R. Soc. London Ser. B **237**, 37 (1952).
5. J. E. Rothenberg, Phys. Rev. A **42**, 682 (1990).
6. P. Kockaert, M. Haelterman, S. Pitois, and G. Millot, Appl. Phys. Lett. **75**, 2873 (1999).
7. G. Millot, S. Pitois, P. Tchofo Dinda, and M. Haelterman, Opt. Lett. **22**, 1686 (1997).
8. S. B. Cavalcanti, J. C. Cressoni, H. R. da Cruz, and A. S. Gouveira-Neto, Phys. Rev. A **43**, 6162 (1991).
9. S. Pitois and G. Millot, Opt. Commun. **226**, 415 (2003).
10. J. D. Harvey, R. Leonhardt, S. Coen, G. Wong, J. C. Knight, W. J. Wadsworth, and P. St. J. Russell, Opt. Lett. **28**, 2225 (2003).
11. S. Coen and M. Haelterman, Phys. Rev. Lett. **79**, 4139 (1997).
12. L. A. Lugiato and R. Lefever, Phys. Rev. Lett. **58**, 2209 (1987).
13. K. Hansen, Opt. Express **11**, 1503 (2003).
14. G. Kozyreff, S. J. Chapman, and M. Tlidi, Phys. Rev. E **68**, 015201(R) (2003).
15. G. Kozyreff and M. Tlidi, Phys. Rev. E **69**, 066202 (2004).